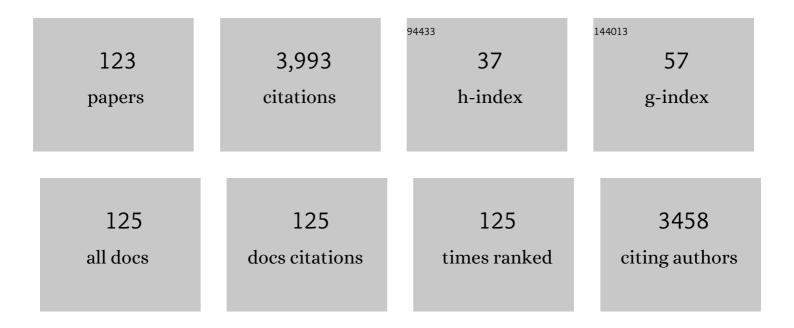
Xiaolu Pang

List of Publications by Year in descending order

Source: https://exaly.com/author-pdf/7248575/publications.pdf Version: 2024-02-01



#	Article	IF	CITATIONS
1	Nickel oxide functionalized silicon for efficient photo-oxidation of water. Energy and Environmental Science, 2012, 5, 7872.	30.8	167
2	The growth mechanism of CO2 corrosion product films. Corrosion Science, 2011, 53, 557-568.	6.6	164
3	Discussion of the CO2 corrosion mechanism between low partial pressure and supercritical condition. Corrosion Science, 2012, 59, 186-197.	6.6	160
4	Insitu grown superhydrophobic Zn–Al layered double hydroxides films on magnesium alloy to improve corrosion properties. Applied Surface Science, 2015, 337, 172-177.	6.1	125
5	Atomic-scale investigation of deep hydrogen trapping in NbC/α-Fe semi-coherent interfaces. Acta Materialia, 2020, 200, 686-698.	7.9	125
6	Mechanical properties of CO2 corrosion product scales and their relationship to corrosion rates. Corrosion Science, 2008, 50, 2796-2803.	6.6	115
7	Effect of small amount of H 2 S on the corrosion behavior of carbon steel in the dynamic supercritical CO 2 environments. Corrosion Science, 2016, 103, 132-144.	6.6	108
8	Formation mechanism and protective property of corrosion product scale on X70 steel under supercritical CO 2 environment. Corrosion Science, 2015, 100, 404-420.	6.6	101
9	Microstructure, residual stress, and fracture of sputtered TiN films. Surface and Coatings Technology, 2013, 224, 120-125.	4.8	100
10	Design and fabrication of enhanced corrosion resistance Zn-Al layered double hydroxides films based anion-exchange mechanism on magnesium alloys. Applied Surface Science, 2017, 404, 246-253.	6.1	95
11	Metal Oxide Composite Enabled Nanotextured Si Photoanode for Efficient Solar Driven Water Oxidation. Nano Letters, 2013, 13, 2064-2072.	9.1	92
12	Brittle film-induced cracking of ductile substrates. Acta Materialia, 2015, 99, 273-280.	7.9	81
13	Corrosion of low alloy steel and stainless steel in supercritical CO 2 /H 2 O/H 2 S systems. Corrosion Science, 2016, 111, 637-648.	6.6	78
14	Cleavage cracking of ductile-metal substrates induced by brittle coating fracture. Acta Materialia, 2018, 152, 77-85.	7.9	73
15	Annealing effects on microstructure and mechanical properties of chromium oxide coatings. Thin Solid Films, 2008, 516, 4685-4689.	1.8	72
16	Film thickness effect on texture and residual stress sign transition in sputtered TiN thin films. Ceramics International, 2017, 43, 11992-11997.	4.8	69
17	The behavior of pre-corrosion effect on the performance of imidazoline-based inhibitor in 3 wt.% NaCl solution saturated with CO 2. Applied Surface Science, 2015, 356, 63-72.	6.1	64
18	One-Step in Situ Synthesis of Reduced Graphene Oxide/Zn–Al Layered Double Hydroxide Film for Enhanced Corrosion Protection of Magnesium Alloys. Langmuir, 2019, 35, 6312-6320.	3.5	63

#	Article	IF	CITATIONS
19	Interfacial Microstructure of Chromium Oxide Coatings. Advanced Engineering Materials, 2007, 9, 594-599.	3.5	56
20	Si photoanode protected by a metal modified ITO layer with ultrathin NiOx for solar water oxidation. Physical Chemistry Chemical Physics, 2014, 16, 4612-4625.	2.8	55
21	Localized CO2 corrosion of carbon steel with different microstructures in brine solutions with an imidazoline-based inhibitor. Applied Surface Science, 2018, 442, 446-460.	6.1	55
22	Effect of flow rate on localized corrosion of X70 steel in supercritical CO2 environments. Corrosion Science, 2018, 136, 339-351.	6.6	55
23	Microstructure and mechanical properties of chromium oxide coatings. Journal of Materials Research, 2007, 22, 3531-3537.	2.6	54
24	Effects of alloyed Cr and Cu on the corrosion behavior of low-alloy steel in a simulated groundwater solution. Corrosion Science, 2016, 102, 114-124.	6.6	54
25	Inhibition of the corrosion of X70 and Q235 steel in CO 2 -saturated brine by imidazoline-based inhibitor. Journal of Electroanalytical Chemistry, 2017, 791, 83-94.	3.8	53
26	Cd-doping a facile approach for better thermoelectric transport properties of BiCuSeO oxyselenides. RSC Advances, 2016, 6, 33789-33797.	3.6	48
27	Corrosion behaviour of low-carbon bainitic steel under a constant elastic load. Corrosion Science, 2010, 52, 3428-3434.	6.6	45
28	Residual stress and microstructure effects on mechanical, tribological and electrical properties of TiN coatings on 304 stainless steel. Ceramics International, 2018, 44, 15851-15858.	4.8	45
29	Investigation of microstructure and mechanical properties of multi-layer Cr/Cr2O3 coatings. Thin Solid Films, 2009, 517, 1922-1927.	1.8	44
30	A novel observation of the interaction between the macroelastic stress and electrochemical corrosion of low carbon steel in 3.5wt% NaCl solution. Electrochimica Acta, 2012, 85, 283-294.	5.2	44
31	Corrosion behavior of each phase in low carbon microalloyed ferrite–bainite dual-phase steel: Experiments and modeling. Corrosion Science, 2013, 75, 67-77.	6.6	44
32	CoCrMo alloy for orthopedic implant application enhanced corrosion and tribocorrosion properties by nitrogen ion implantation. Applied Surface Science, 2015, 347, 23-34.	6.1	44
33	The relationship between fracture toughness of CO2 corrosion scale and corrosion rate of X65 pipeline steel under supercritical CO2 condition. International Journal of Greenhouse Gas Control, 2011, 5, 1643-1650.	4.6	41
34	Temperature, moisture and mode-mixity effects on copper leadframe/EMC interfacial fracture toughness. International Journal of Fracture, 2014, 185, 115-127.	2.2	41
35	Corrosion of low alloy steel containing 0.5% chromium in supercritical CO2-saturated brine and water-saturated supercritical CO2 environments. Applied Surface Science, 2018, 440, 524-534.	6.1	40
36	Microstructure evolution of in-situ nanoparticles and its comprehensive effect on high strength steel. Journal of Materials Science and Technology, 2019, 35, 1940-1950.	10.7	40

#	Article	IF	CITATIONS
37	Brittle coating effects on fatigue cracks behavior in Ti alloys. International Journal of Fatigue, 2019, 125, 432-439.	5.7	40
38	Residual Stress and Surface Energy of Sputtered TiN Films. Journal of Materials Engineering and Performance, 2015, 24, 1185-1191.	2.5	39
39	Improved thermoelectric performance of BiCuSeO by Ag substitution at Cu site. Journal of Alloys and Compounds, 2017, 691, 572-577.	5.5	38
40	Role of deposition parameters on microstructure and mechanical properties of chromium oxide coatings. Surface and Coatings Technology, 2007, 202, 58-62.	4.8	37
41	Structure and composition effects on electrical and optical properties of sputtered PbSe thin films. Thin Solid Films, 2015, 592, 59-68.	1.8	36
42	Discontinuous surface cracks during stress corrosion cracking of stainless steel single crystal. Corrosion Science, 2011, 53, 3509-3514.	6.6	35
43	Corrosion behavior of steel with different microstructures under various elastic loading conditions. Corrosion Science, 2013, 75, 293-299.	6.6	35
44	Porosity dependence of elastic modulus of porous Cr3C2 ceramics. Ceramics International, 2014, 40, 191-198.	4.8	35
45	Characterization of microstructure evolution after severe plastic deformation of pure copper with continuous columnar crystals. Materials Science & Engineering A: Structural Materials: Properties, Microstructure and Processing, 2010, 527, 4750-4757.	5.6	32
46	The effect of ion implantation on tribology and hot rolling contact fatigue of Cr4Mo4Ni4V bearing steel. Applied Surface Science, 2014, 305, 93-100.	6.1	31
47	Study on the growth mechanism and optical properties of sputtered lead selenide thin films. Applied Surface Science, 2015, 356, 978-985.	6.1	30
48	Effects of substrate bias voltage on mechanical properties and tribological behaviors of RF sputtered multilayer TiN/CrAlN films. Journal of Alloys and Compounds, 2016, 665, 210-217.	5.5	30
49	Enhanced thermoelectric efficiency of Cu2â^'Se–Cu2S composite by incorporating Cu2S nanoparticles. Ceramics International, 2016, 42, 8395-8401.	4.8	30
50	Interface and Strain Energy Revolution Texture Map To Predict Structure and Optical Properties of Sputtered PbSe Thin Films. ACS Applied Materials & Interfaces, 2016, 8, 625-633.	8.0	29
51	High temperature brittle film adhesion measured from annealing-induced circular blisters. Acta Materialia, 2017, 138, 1-9.	7.9	29
52	Effect of exposure angle on the corrosion behavior of X70 steel under supercritical CO 2 and gaseous CO 2 environments. Corrosion Science, 2017, 121, 57-71.	6.6	28
53	Passive film-induced stress and mechanical properties of α-Ti in methanol solution. Corrosion Science, 2014, 78, 287-292.	6.6	27
54	Atomic-scale insights on hydrogen trapping and exclusion at incoherent interfaces of nanoprecipitates in martensitic steels. Nature Communications, 2022, 13, .	12.8	27

#	Article	IF	CITATIONS
55	Study of the stability of α-Fe/MnS interfaces from first principles and experiment. Applied Surface Science, 2020, 501, 144017.	6.1	26
56	Corrosion resistance and friction of sintered NdFeB coated with Ti/TiN multilayers. Thin Solid Films, 2014, 550, 428-434.	1.8	24
57	Corrosion behaviors of steels under supercritical CO2 conditions. Corrosion Reviews, 2015, 33, 151-174.	2.0	24
58	Characterization of corrosion products formed on different surfaces of steel exposed to simulated groundwater solution. Applied Surface Science, 2015, 345, 10-17.	6.1	24
59	Stress-sensitive fatigue crack initiation mechanisms of coated titanium alloy. Acta Materialia, 2021, 217, 117179.	7.9	24
60	Investigation on hydrogen induced cracking behaviors of Ni-base alloy. International Journal of Hydrogen Energy, 2011, 36, 5729-5738.	7.1	23
61	Characterization of the mechanical properties and failure modes of hard coatings deposited by RF magnetron sputtering. Surface and Coatings Technology, 2008, 202, 3354-3359.	4.8	22
62	Effect of surface roughness on the performance of thioureido imidozaline inhibitor in CO2-saturated brine. Corrosion Science, 2019, 157, 189-204.	6.6	22
63	Mechanical properties and phases evolution in T91 steel during long-term high-temperature exposure. Engineering Failure Analysis, 2020, 111, 104451.	4.0	21
64	Influence of temperature field on the microstructure of low carbon microalloyed ferrite–bainite dual-phase steel during heat treatment. Materials Science & Engineering A: Structural Materials: Properties, Microstructure and Processing, 2012, 536, 136-142.	5.6	19
65	Water molecules effect on pure Ti passive film structure in methanol solution. Applied Surface Science, 2014, 303, 282-289.	6.1	19
66	Comparative study of Ti and Cr adhesion to the AlN ceramic: Experiments and calculations. Applied Surface Science, 2018, 457, 856-862.	6.1	19
67	Residual stress control in CrAlN coatings deposited on Ti alloys. Ceramics International, 2018, 44, 4653-4659.	4.8	18
68	Electrochemical Oxidation of Methanol on Pt-SnO _x /C Catalysts Characterized by Electrochemical Society, 2015, 162, F1540-F1548.	2.9	17
69	Pronounced effect of ZnTe nanoinclusions on thermoelectric properties of Cu2â^x Se chalcogenides. Science China Materials, 2016, 59, 135-143.	6.3	17
70	Effects of orientation on microstructure and mechanical properties of TiN/AlN superlattice films. Scripta Materialia, 2021, 201, 113951.	5.2	17
71	Fast deposition of diamond-like carbon films by radio frequency hollow cathode method. Thin Solid Films, 2013, 534, 226-230.	1.8	16
72	Failure analysis of the oil transport spiral welded pipe. Engineering Failure Analysis, 2012, 25, 169-174.	4.0	15

#	Article	IF	CITATIONS
73	First principles calculations of interfacial properties and electronic structure of the AlN(0 0 0 1)/Ti(0 0 0 1) interface. Chemical Physics Letters, 2018, 713, 153-159.	2.6	15
74	Interaction between Cu and Cr coadsorption on MnS inclusions in low alloy steels. Applied Surface Science, 2019, 471, 425-434.	6.1	15
75	AlTiN layer effect on mechanical properties of Ti-doped diamond-like carbon composite coatings. Thin Solid Films, 2011, 519, 5353-5357.	1.8	14
76	Annealing effects on microstructure and mechanical properties of sputtered multilayer Cr(1â^'x)AlxN films. Thin Solid Films, 2011, 519, 5831-5837.	1.8	14
77	Thermodynamic energy variation diagram to speculate preferred growth orientation of magnetron sputtered PbSe thin films on monocrystalline silicon substrates. Applied Surface Science, 2018, 452, 1-10.	6.1	14
78	TiN-Coating Effects on Stainless Steel Tribological Behavior Under Dry and Lubricated Conditions. Journal of Materials Engineering and Performance, 2014, 23, 1263-1269.	2.5	13
79	Mechanical properties of a bi-continuous Cu–Cr3C2 composite. Materials Science & Engineering A: Structural Materials: Properties, Microstructure and Processing, 2015, 623, 4-9.	5.6	12
80	Crevice corrosion of copper for radioactive waste packaging material in simulated groundwater. Corrosion Engineering Science and Technology, 2016, 51, 11-17.	1.4	12
81	Electrical conductivity and wear behavior of bi-continuous Cr3C2–Cu composites. Ceramics International, 2015, 41, 11075-11079.	4.8	11
82	Thickness effect on the band gap of magnetron sputtered Pb45Se45O10 thin films on Si. Physica E: Low-Dimensional Systems and Nanostructures, 2015, 67, 152-158.	2.7	11
83	In-situ stress gradient evolution and texture-dependent fracture of brittle ceramic thin films under external load. Ceramics International, 2018, 44, 8176-8183.	4.8	11
84	Formation of high-density stacking faults in ceramic films induced by Ti transition layer. Scripta Materialia, 2022, 211, 114496.	5.2	11
85	Adhesion of Sputtered Nickel Films on Polycarbonate Substrates. Journal of Materials Engineering and Performance, 2014, 23, 786-790.	2.5	10
86	First principles calculations study of crystallographic orientation effects on SiC/Ti and SiC/Cr interfaces. Microelectronics Reliability, 2018, 83, 119-126.	1.7	10
87	Synergistic effect of Cu and Cr on pitting behavior induced by MnS inclusions in low alloy steels. Journal of Alloys and Compounds, 2021, 864, 158133.	5.5	10
88	Room temperature ferromagnetism in sputtered Zn1â^'xCrxO thin films. Materials Letters, 2011, 65, 2728-2730.	2.6	9
89	Nitrogen effects on structure, mechanical and thermal fracture properties of CrN films. Ceramics International, 2021, 47, 30729-30740.	4.8	9
90	Thickness effects on optical and photoelectric properties of PbSeTeO quaternary thin films prepared by magnetron sputtering. Journal of Materials Science: Materials in Electronics, 2015, 26, 7873-7881.	2.2	8

#	Article	IF	CITATIONS
91	Substrate slip steps promote cracking and buckling of thin brittle film. Scripta Materialia, 2019, 163, 82-85.	5.2	8
92	Fracture Toughness and Adhesion of Transparent Al:ZnO Films Deposited on Glass Substrates. Journal of Materials Engineering and Performance, 2013, 22, 3161-3167.	2.5	7
93	Failure analysis of high nickel alloy steel seal ring used in turbomachinery. Engineering Failure Analysis, 2017, 80, 49-56.	4.0	7
94	Review of metal carbide nanoprecipitate effects on hydrogen embrittlement of high strength martensitic steel. Anti-Corrosion Methods and Materials, 2022, 69, 409-416.	1.5	7
95	Hydrogen trapping and hydrogen embrittlement in 15-5PH stainless steel. Corrosion Science, 2022, 205, 110416.	6.6	7
96	Annealing temperature effects on optical and photoelectric properties of sputtered indium-doped PbSe thin films. Journal of Materials Science: Materials in Electronics, 2016, 27, 1670-1678.	2.2	6
97	Externally applied stress sign and film elastic properties effects on brittle film fracture. Philosophical Magazine, 2016, 96, 447-458.	1.6	6
98	High stress corrosion cracking resistance of in-situ nanoparticle strengthened steel. Corrosion Communications, 2022, 5, 14-24.	6.0	6
99	Surface Potential Distribution in an Indentation―Pre racked <scp>BaTiO₃</scp> Single Crystal. Journal of the American Ceramic Society, 2011, 94, 4299-4304.	3.8	5
100	Investigation of corrosion behaviours of high level waste container materials in simulated groundwater in China. Corrosion Engineering Science and Technology, 2014, 49, 480-484.	1.4	5
101	Development and application of metalÂmaterials in terms of vascular stents. Bio-Medical Materials and Engineering, 2015, 25, 435-441.	0.6	5
102	Applications and Thermodynamic Analysis of Equilibrium Solution for Secondary Phases in Ti–N–C Gear Steel System with Nano-Particles. Metals, 2017, 7, 110.	2.3	5
103	Thermodynamics Analysis of Multiple Microelements' Coupling Behavior in High Fatigue Resistance 50CrVA Spring Steel with Nanoparticles. Materials, 2019, 12, 2952.	2.9	5
104	Tribo-corrosion and Albumin Attachment of Nitrogen Ion-Implanted CoCrMo Alloy During Friction Onset. Journal of Materials Engineering and Performance, 2019, 28, 363-371.	2.5	5
105	Thermal-induced blister cracking behavior of annealed sandwich-structured TiN/CrAlN films. Ceramics International, 2018, 44, 5874-5879.	4.8	4
106	Thermodynamic Analysis of Ti3O5Nanoparticles Formed in Melt and Their Effects on Ferritic Steel Microstructure. Materials, 2018, 11, 1343.	2.9	4
107	Discontinuous cracking of TiN films on a steel substrate induced by an adhesive interlayer. Philosophical Magazine Letters, 2019, 99, 199-207.	1.2	4
108	Moisture Effects on Gold Nanowear. Materials Research Society Symposia Proceedings, 2008, 1085, 51001.	0.1	3

#	Article	IF	CITATIONS
109	Microstructure and mechanical properties of Ti/AlTiN/Ti-diamondlike carbon composite coatings on steel. Journal of Materials Research, 2010, 25, 2159-2165.	2.6	3
110	Surface carbon chemical states of ion implanted AISI 440C martensitic stainless steel. Journal of Iron and Steel Research International, 2015, 22, 513-518.	2.8	3
111	The Effect of Exposure Angle on the Corrosion Behavior of Low-Carbon Microalloyed Steel Under CO2Conditions. Corrosion, 2015, 71, 343-351.	1.1	3
112	Effects of anions on corrosion behaviour of carbon steel in simulated groundwater in China. Corrosion Engineering Science and Technology, 2017, 52, 84-89.	1.4	3
113	Selection of interfacial metals for Si3N4 ceramics by the density functional theory. Chemical Physics Letters, 2021, 763, 138189.	2.6	2
114	High-throughput technique for stress corrosion cracking susceptibility measurements based on film-induced stress. Vacuum, 2022, 203, 111275.	3.5	2
115	Analysis and Measurement of Forces in an Electrowetting-Driven Oscillator. Materials Research Society Symposia Proceedings, 2007, 1052, 1.	0.1	1
116	Mechanical Properties of Evaporated Gold Films. Hard Substrate Effect Correction. Materials Research Society Symposia Proceedings, 2008, 1086, 1.	0.1	1
117	Achieving Low Yield Ratio in Highâ€Strength Steel by Tuning Multiple Microstructures. Steel Research International, 0, , 2100415.	1.8	1
118	Pattern Formation During Nanowear of Gold Films. Materials Research Society Symposia Proceedings, 2007, 1059, 1.	0.1	0
119	Substrate Roughness Effects on Chromium Oxide Coating Adhesion and Wear Resistance. Advanced Materials Research, 2010, 97-101, 1261-1264.	0.3	0
120	Annealing Temperature Effect on the Microstructure and Adhesion of SiC Films Produced by MF Magnetron Sputtering. Advanced Materials Research, 2011, 287-290, 2423-2428.	0.3	0
121	Failure Analysis of Differential Pressure Transmitter Impulse Pipe in High Sulfur Purification Device. Applied Mechanics and Materials, 2014, 668-669, 102-106.	0.2	0
122	Deformation Mechanisms of NiP/Ni Composite Coatings on Ductile Substrates. Coatings, 2021, 11, 834.	2.6	0
123	Fabrication of a Superhydrophobic Film with Self-Cleaning Property on Magnesium Alloy and its Corrosion Resistance Properties. , 2016, , 279-283.		Ο